redin Revista Facultad de Ingeniería, Universidad de Antioquia, No.112, pp. 86-97, Jul-Sep 2024

Titania modifications with fluoride, sulfate, and platinum for photochemical reduction of chromium (VI)

Titania modificada con fluoruro, sulfatos y platino para la reducción fotoquímica de cromo (VI)

Julie Joseane Murcia [1], **Mónica Sirley Hernández-Laverde** [1, 2*], **Ivan Alexander Correa-Camargo** [1], **Hugo Alfonso Rojas-Sarmiento** [1], **José Antonio Navío** [3], **Maria del Carmen Hidalgo-López** [3]

[1]Grupo de Catálisis, Escuela de Ciencias Químicas, Universidad Pedagógica y Tecnológica de Colombia UPTC. Avenida Central del Norte. C. P. 150003. Tunja, Boyacá, Colombia.
[2]Grupo GIA, Escuela de Ciencias Básicas Tecnología e Ingeniería. Universidad Nacional Abierta y a Distancia UNAD. Calle 5 #1A-52. C. P. 152217. Boyacá, Colombia.
[3]Instituto de Ciencia de Materiales de Sevilla (ICMS), Consejo Superior de Investigaciones Científicas CSIC. Universidad de Sevilla. Américo Vespucio 49, 41092. Seville, Spain.

CITE THIS ARTICLE AS:

J. J. Murcia, M. S. Hernández-Laverde, I. A. Correa-Camargo, H. A. Rojas-Sarmiento, J. A. Navío, M. del C. Hidalgo-López. "Titania modifications with fluoride, sulfate, and platinum for photochemical reduction of chromium (VI)", *Revista Facultad de Ingeniería Universidad de Antioquia*, no. 112, pp. 86-97, Jul-Sep 2024. [Online]. Available: https://www.doi.org/10.17533/udea.redin.20240304

ARTICLE INFO:

Received: March 13, 2023
Accepted: March 08, 2024
Available online: March 08, 2024

KEYWORDS:

$F-TiO_2$; $S-TiO_2$; $Pt-F-TiO_2$; $Pt-S-TiO_2$; chromium, photoreduction.

$F-TiO_2$; $S-TiO_2$; $Pt-F-TiO_2$; $Pt-S-TiO_2$; Cromo, fotoreducción.

ABSTRACT: In this work, Titania was modified by sulfation or fluorination and platinum on the surface to improve the Cr (VI) reduction efficiency compared to the bare TiO_2 material synthesized by the sol-gel method. The synthesized materials were characterized by XRD, S_{BET}, UV-Vis DRS, XRF, TEM, FTIR, and XPS. The modifications led to higher stability in the Anatase phase and surface area of this semiconductor. The addition of F and Pt in TiO_2 led to absorption increases in the visible region of the electromagnetic spectrum. A correlation between the new physicochemical properties obtained after TiO_2 modification and the photocatalytic performance of this material was observed. The best result in chromium reduction was obtained using Pt-S-TiO_2 as the photocatalyst; this material showed a suitable combination of surface area, high UV-Vis absorption, high hydroxylation, and the existence of Pt nanoparticles on the surface, which favors an increased electron-hole pair half-life. Different reaction parameters were also evaluated, which demonstrated that the best photocatalytic performance was obtained under an N_2 atmosphere, a light intensity of 120 W/m^2, and 2 hours of total reaction time. Likewise, it was noted that an increase in reaction time from 2 to 5 hours, had a detrimental effect on reducing Cr (VI) efficiency.

RESUMEN: En este trabajo, la Titania se modificó por sulfatación o fluorización y platino en superficie, con el objetivo de mejorar la eficiencia en la reducción de Cr (VI) en comparación con el material TiO_2 base sintetizado por el método sol-gel. Los materiales fueron caracterizados por DRX, S_{BET}, UV-Vis DRS, FRX, TEM, FTIR y XPS. Las modificaciones permitieron obtener una mayor estabilidad en la fase Anatasa y en el área superficial del semiconductor. La adición de F y Pt en el TiO_2 provocaron aumentos de absorción en la región visible del espectro electromagnético. Se observó una correlación entre las nuevas propiedades fisicoquímicas obtenidas tras la modificación del TiO_2 y el rendimiento fotocatalítico del material. El mejor resultado en la reducción de cromo se obtuvo utilizando Pt-S-TiO_2 como fotocatalizador, este material mostró una combinación adecuada de área superficial, alta absorción UV-Vis, alta hidroxilación y la existencia de nanopartículas de Pt en la superficie que favorecen un aumento de la vida media del par electrón-hueco. También se evaluaron parámetros de reacción que demostraron que el mejor desempeño fotocatalítico se obtuvo bajo atmósfera de N_2, intensidad de luz de 120 W/m^2 y 2 horas de tiempo total de reacción. Así mismo, se observó que aumentar el tiempo de reacción de 2 a 5 horas tuvo un efecto perjudicial sobre la eficiencia en la reducción de Cr (VI).

* Corresponding author: Mónica Sirley Hernández-Laverde
E-mail: monica.hernandez06@uptc.edu.co
ISSN 0120-6230
e-ISSN 2422-2844

DOI: 10.17533/udea.redin.20240304

1. Introduction

Heavy metal pollution currently represents a critical concern around the world; these pollutants, coming from different industrial activities, have been reaching natural water sources [1]. Latin American countries have usually employed conventional technologies for the treatment of wastewater. These processes can eliminate many pollutants, but heavy metals can be persistent contaminants [1–3].

For decades, several strategies have been employed for the removal of metals, such as (i) ion exchange and separation by membranes [1, 4], which can be costly treatments, while (ii) precipitation and adsorption [2, 5], led to residual sludges production. Therefore, conventional techniques should not be considered definitive treatments and result in a necessary search for new and more effective alternatives for recovering heavy metals from wastewater.

Hexavalent chromium was selected as the model metal in the current work. This element of anthropogenic origin is produced by the petroleum industry and is used in the manufacture of paint, as a wood preservative, in steel production, in electronic devices, for metals finishing, in tanneries, the textile industry, and in the manufacture of corrosion inhibitors [6]. This metal represents a risk to human health and is in the group of carcinogenic compounds classified by the International Agency for Research on Cancer (IARC) [6, 7]. In the human body, chromium is absorbed in cells. It can be reduced intracellularly in mitochondria, which takes place by intercellular reducers, thus generating free chromium (V and VI) and hydroxyl radical species.

Heterogeneous photocatalysis currently represents a good alternative for heavy metal removal from wastewater. During the photocatalytic process, the photochemical reduction of metals takes place on the semiconductor surface as the result of photogenerated electrons [8, 9]. Unlike other conventional treatments, photocatalytic removal may give a new life for some metals. As a result, the photoreduced elements on the semiconductor surface can contribute to obtaining new photocatalytic materials that could be employed in environmental remediation reactions induced by bimetallic photocatalysts [10]. Chemical photoreduction techniques have been extensively used in our research group and by other researchers for photocatalyst synthesis [11, 12], where interesting results have been obtained for the treatment of contaminants.

Different authors have reported the removal of chromium by using photocatalytic processes [13–15]. Photocatalytic reduction of chromium with the use of an electron donor or sacrificial agent has also been reported [16]. In the current study, TiO_2-based photocatalysts were employed and modified by fluoridation, sulfation, and platinum addition in order to improve the efficiency of these semiconductors. Additionally, the effect of different reaction parameters was also evaluated. In general, it was found that fluoridation and platinization of TiO_2 led to the generation of effective materials for Cr removal from the liquid phase. It has been determined that the photocatalytic reaction time is a determinant factor in limiting the effectiveness of global metal photoreduction.

2. Experimental procedure

2.1 Photocatalysts preparation

TiO_2 **sol-gel** was obtained by controlled hydrolysis of titanium tetraisopropoxide (Aldrich, 97%) in an isopropanol solution (volume ratio isopropanol/water 1:1). The powder material was filtered and dried at 120°C for 12 hours. Afterwards, a portion of this material was calcinated at 650°C for 2 hours using a heating ramp of 4°C/min [17]. Commercial TiO_2 Sigma Aldrich was used as the reference material.

Fluoridation was performed by immersing the uncalcined TiO_2 powder in a 10 mM solution of NaF. The pH value selected for the fluoridation process was 3.0, facilitating the anchoring of fluorine ions on the titania surface. The solution used to control pH was 1M HCl. This suspension was left under continuous stirring for 1 hour, then filtered, dried, and calcinated at 650°C for 2 hours using a heating ramp of 4°C/min to obtain $F - TiO_2$ [17, 18].

Sulfonation was obtained by suspending uncalcined TiO_2 sol-gel powder in a 1M H_2SO_4 solution. This suspension was left under continuous stirring for 1 h. After this, the solid was filtrated, dried, and calcinated at 650°C for 2 hours using a heating ramp of 4°C/min to obtain $S - TiO_2$ [17, 18].

The platinum addition on bare, sulfated, and fluorinated TiO_2 was carried out using photochemical reduction. A suspension of these materials in a solution of the metal precursor was prepared (5g of each photocatalyst per liter of $H_2PtCl_6.6H_2O$). 0.5% of the total weight of TiO_2 was the nominal amount of Pt selected for this work. In this process, a solution of 0.3 M isopropanol was employed as an electron donor.

The Pt photodeposition was performed in a batch Pyrex reactor wrapped in aluminum foil under illumination for 2 hours with an intensity of 60 W/m^2, which was measured using a Delta OHM HD 2102.2 photoradiometer.

A continuous flow of N_2 was employed to maintain an inert atmosphere inside the reactor. Finally, the photocatalysts were filtered and dried at 120°C for 12 hours. The materials synthesized were labeled as Pt-F-TiO_2 and Pt-S-TiO_2 [17, 18].

2.2 Photocatalysts characterization

A complete characterization of the photocatalysts prepared was performed, and the analysis for each instrumental technique was previously reported in different studies [17–21]. A general description of the equipment employed for this analysis is presented as follows:

The crystalline phase composition of the prepared materials was analyzed using a Philips PW1700 diffractometer.

Measurements of the Specific surface area S_{BET} were performed in a Micromeritics ASAP 2010 instrument.

The UV-Vis DRS was recorded on a Varian spectrophotometer (model Cary 100).

X-Ray Fluorescence (XRF) spectrometry was used to find the chemical composition of the solids in a Panalytic Axios sequential spectrometer.

Morphology analysis and distribution of particles within the materials were carried out in a Philips CM200 microscope.

The Infrared spectroscopy analysis was performed using a Thermo Scientific Nicolet iS50 spectrometer.

X-ray photoelectron spectroscopy (XPS) analysis was performed with a Leybold–Heraeus LHS-10 spectrometer.

2.3 Chromium (VI) chemical photoreduction tests

Each of the synthesized photocatalysts was tested in the reaction of photochemical reduction of chromium. The reaction conditions employed in this study are described as follows:

- *Starting solution:* 100 mL of a 0.4 mM solution of $K_2Cr_2O_7$.
- *Photocatalyst loading*: 1g/L.
- *Reactor:* A 100 mL batch Pyrex reactor with a water flow cooling system to keep the temperature at 24°C.
- *Light source:* An Osram Ultra-Vitalux lamp (300W) with a sun-like radiation spectrum in UVA and UVB.
- *Light intensity:* 30 and 120 W/m^2
- *Reaction atmosphere:* Constant nitrogen flow of 0.84L/h or constant oxygen flow of 0.84L/h.
- *Total reaction time:* 2 to 5 hours.
- *Sampling:* The Cr concentration was monitored by taking aliquots from the reactor at different periods: 0, 2, 5, 10, 15, 30, 45, 60, 90, and 120 min.
- *Adsorption-desorption balance:* The reaction suspension was homogenized by ultrasound for 10 min before the lamp was switched on.

To determine the actual effectiveness of the photocatalytic process, two blank reactions were carried out:

- **i)** *Direct UV-Vis light effect:* Firstly, the $K_2Cr_2O_7$ solution was maintained under continuous illumination and stirring without a photocatalyst.
- **ii)** *Cr adsorption test:* the suspension of each photocatalyst in the $K_2Cr_2O_7$ solution was maintained in the dark under continuous stirring.

To ensure the repeatability of the photocatalytic treatment, duplicate trials were performed for each reaction, which found an error percentage of 0.1%.

Determination of chromium (VI) concentration

The variation in Cr (VI) concentration was determined by the 1,5-diphenylcarbazide (DPC) method at 542 nm [22]. For the spectrophotometric evaluations, a Thermo Scientific Evolution 300 UV-Vis spectrophotometer was used. Prior to the UV-Vis analysis, a pre-treatment was carried out on the samples. A colorimetric method that consisted of the addition of 1,5-diphenylcarbazide in an acid medium was used. This compound bound to Cr (VI) produces a violet color in the solution. The initial and final concentrations of each sample were taken into account to determine the percentage of chromium (VI) removal during the 2 hours of reaction.

Determination of total chromium content

The samples taken from the liquid phase during the reactions were examined before and after photocatalytic evaluation by using two methods described in the Standard Methods for Examination of Water and Wastewater: SM 3111B and 3113B. By following these methodologies, the Atomic Absorption Spectrometry techniques were determined in a Shimadzu AA-7000 spectrometer [23]. For this analysis, the flame atomization from air-acetylene combustion and a gas flow of 2.8 L/min were used. The light source used was a hollow cathode Cr/Ni model BGC-D2 lamp, and the wavelength selected for Cr determination was 357.9 nm.

Finally, to determine the real photochemical reduction or adsorption of chromium on the surface of the photocatalytic material, each of them was analyzed by XPS. From this technique, it was possible to identify the changes in the oxidation state of this chemical element. XPS analysis was performed using aluminum anodes as an X-ray source, using a constant step energy of 100 eV. The scale was corrected using the binding energy (BE) of the spectra by reference to the C- (C, H) component at 284.8 eV of the C 1s peak.

3. Results

3.1 Photocatalysts characterization

In general, the characterization results of the photocatalysts analyzed have been previously reported by our research group [17–21]. To compare the data in the current study, we included a summary of the main results as follows:

XRD: Figure 1 shows the XRD patterns of all photocatalysts; it was observed that crystalline phases Anatase and Rutile coexist only in TiO_2 Sol-gel identified by their characteristic peaks located at the 2 theta positions of 25.23 and 27.33, respectively, the modified photocatalysts seem to be exclusive to the crystalline phase Anatase, possibly owing to the protective effect of F- and SO_4^{-2} on the surface of TiO_2 during the calcination process [17, 21]. The photodeposition of Pt nanoparticles during the process of preparing materials did not modify the composition of the crystalline phases of TiO_2 [24].

In Table 1, it was noted that the values of the anatase crystallite sizes increased after the sulfation and fluoridation treatments. It has been reported that the presence of F- ions improves the crystallinity of the titania and allows the anatase crystals to be larger [19].

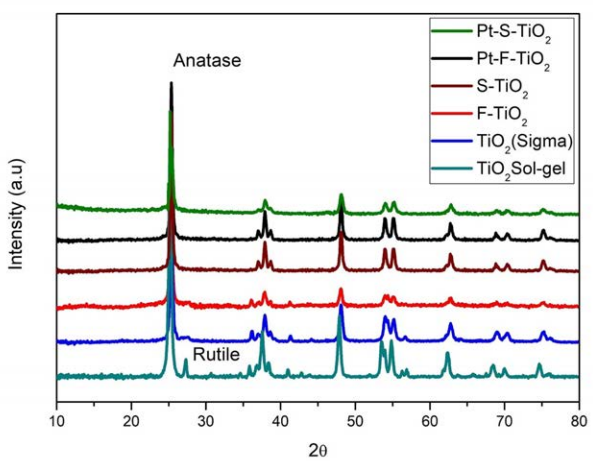

Figure 1 XRD patterns for all photocatalysts

S_{BET} The lowest values in specific surface area corresponded to the TiO_2 sol-gel due to the particles sintering in the calcination stage to 650°C (Table 1). In the S-TiO_2 and F-TiO_2 materials, the surface area value significantly increases, which agrees with the protective nature of the sulfate and fluorine species on the TiO_2 surface during calcination, inhibiting the agglomeration of particles [25]. It was also observed that after platinization, the surface area decreases, which may be caused by the obstruction of the TiO_2 pores by Pt nanoparticles [17].

UV-Vis DRS: Band gap values of the photocatalysts calculated from UV-Vis DRS analysis show small decreases in these values after sulfation, fluoridation, and platinization, as observed in Table 1. UV-Vis DR spectra of all photocatalysts are presented in Figure 2; the characteristic absorption edge of TiO_2 at around 360-380 nm can be seen for all samples. A slight absorption shift towards the visible region of the electromagnetic spectrum can also be observed for fluorinated and platinized photocatalysts; this is due to the presence of fluoride ions (F-) on the TiO_2 surface [26], and in the case of platinized materials due to the gray coloration of the powders attributed to the presence of Pt^0 species on the surface.

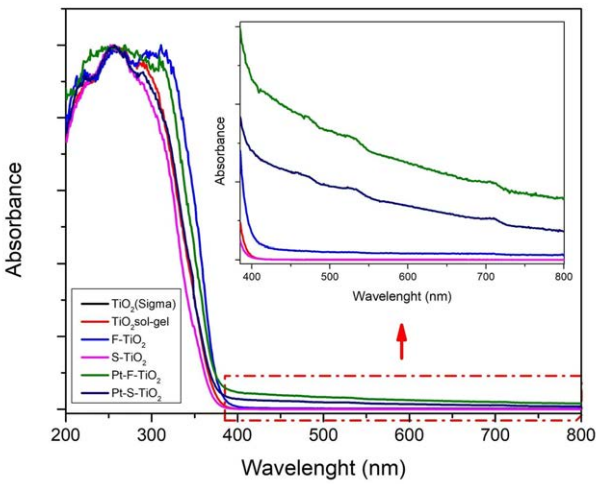

Figure 2 UV-Vis DR spectra of all photocatalysts

XRF: From the XRF analysis, it was possible to determine that the real amount of platinum present in the samples was 0.25 wt.% for Pt-F-TiO_2 and 0.25 wt.% for Pt-S-TiO_2. These values are lower than the nominal 0.5 wt.%. Traces of chloride ions that came from the metal precursor were also found (Table 1).

TEM: In Figure 3, TEM micrographs of the platinized samples are shown, where it is possible to observe small dark and spherical Pt particles, which are placed on the anatase surface. The histograms in Figure 3 represent the Pt particle size distribution. As seen in the Pt-F-TiO_2 (Fig. 3a) sample, the Pt particles are distributed in a more heterogeneous way compared with Pt-S-TiO_2 (Fig. 3b). The average metal particle size was > 6 nm for fluorinated photocatalysts and between 6-7 nm for sulfated photocatalysts. The highest dispersion of platinum on the sulfated photocatalyst could be due to its surface area, which is higher than that observed for

Table 1 Main photocatalysts characterization results

Photocatalysts	$D_{anatase}$ (nm)	S_{BET} (m^2/g)	Band gap (eV)	Binding energy (eV)		O/Ti	XRF (wt.%)
				Ti $2p_{3/2}$	O 1s		
TiO_2(Sigma)	22	51	3.23	458.5	529.8	1.87	-
TiO_2 sol-gel	17	11	3.30	458.5	529.8	1.96	-
$S-TiO_2$	20	58	3.20	458.5	529.8	1.70	-
$F-TiO_2$	24	51	3.21	458.4	529.6	2.00	-
$Pt-S-TiO_2$	20	49	3.20	458.4	529.6	1.88	0.25 (Pt) 0.03 (Cl^-)
$Pt-F-TiO_2$	23	42	3.24	458.4	529.8	2.06	0.25 (Pt) 0.05 (Cl^-)

Pt-F-TiO_2 (Table 1). The presence of oxygen vacancies in the sulfated solid can also contribute to the homogeneous distribution of Pt [9].

FTIR: Infrared spectroscopy analysis allowed the identification of OH-isolated groups, H-bonded hydroxyl groups, Ti-OH interactions, and Ti-OH_2 interactions coming from water adsorbed on the TiO_2 surface [27].

XPS: Figure 4a shows the XPS analysis in the O 1s region with a signal located at 529.8 eV corresponding to the surface O2- species present in all photocatalysts as reported in Table 1. As it can be seen, the TiO_2 sol-gel does not present a shoulder; however, when the sulfation and fluoridation process was performed, an evident shoulder located at 532 eV was observed, thus demonstrating the existence of OH- groups on the surface. The highest intensity of this shoulder observed in F-TiO_2 and S-TiO_2 photocatalysts may indicate a higher degree of hydroxylation in these materials, mainly due to the presence of oxygen vacancies. After platinum addition, the shoulder disappears: it is because the platinum on the surfaces attracts these electronegative groups to generate the photochemical reduction, thus changing the chemical environment and decreasing the hydroxylation on the surface for the Pt-F-TiO_2 and Pt-S-TiO_2.

The fluorinated photocatalysts were analyzed by XPS, and in the F 1s region, the main signal located at 684 eV in Figure 4b corresponds to fluoride ions present on the surface as $\equiv$ Ti-F species. In the fluorinated samples, an exchange of ligands between the F- and OH- on the TiO_2 surface ($\equiv \mathrm{Ti-OH}$) [28] exists. A decrease in the intensity of the fluorine signal was also observed after platinization: this is because the highly electronegative fluoride groups contribute to the photochemical reduction of Pt2+ to Pt0 so that the degree of surface fluoridation decreases in the Pt-F-TiO_2. The atomic content of fluorine was 1.83% for F-TiO_2 and 1.12 % for Pt-F-TiO_2.

As can be seen in Figure 4c, the $\mathrm{TTi2p_{3/2}}$ region in TiO_2 is very similar for all samples, with peaks centered at binding energies of 458.5±0.2 eV. This value is assigned to $\mathrm{Ti^{4+}}$ species present in the lattice of TiO_2 as the main component: this indicates that the chemical environment of titanium was unchanged after modification by sulfation, fluoridation, or platinization.

Table 1 reports that the O/Ti atomic ratio estimated for the samples analyzed is lower than the stoichiometric value O/Ti=2, proving the presence of certain oxygen vacancies on the surface of this oxide. S-TiO_2 showed the lowest O/Ti ratio of 1.70. This result agrees with what has been found in previous studies, where it is indicated that the pre-treatment of TiO_2 with sulfuric acid and subsequent calcination at high temperature (> 600 ºC) results in a surface rich in oxygen vacancies [29]. In the case of Pt-S-TiO_2 photocatalysts, the ratio O/Ti increases to 1.88, suggesting that oxygen vacancies were partially removed during the photodeposition process.

Figure 5 shows the spectra obtained for Pt $\mathrm{4f_{7/2}}$ and Pt $\mathrm{4f_{5/2}}$ in the Pt-S-TiO_2 photocatalyst. From these spectra, it is possible to observe that in the platinized materials, species of oxidized and reduced Pt coexist. This can be seen by the characteristic doublets of these species located at 71 eV and 72.4 eV for Pt0 and Pt2+, respectively. These results indicate that platinum was not completely reduced on the TiO_2 surface, as evidenced by the XRF analysis presented above.

The Pt-S-TiO_2 sample was selected for XPS analysis before (Figure 5a) and after (Figure 5b) chromium reduction reactions. From this analysis, it was possible to determine that this material presents high stability after photocatalytic reaction, with no modifications in the Pt 4f region being observed.

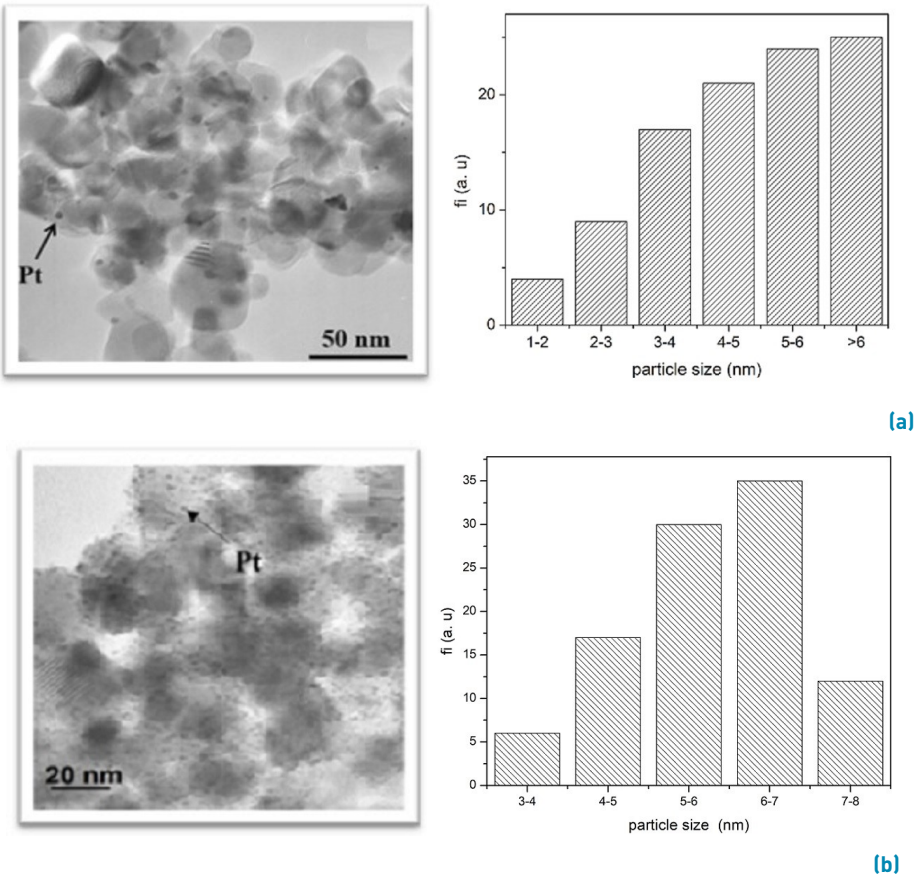

Figure 3 TEM micrographs of platinized materials. (a) Pt-F-TiO_2 and b) Pt-S-TiO_2

3.2 Photochemical reduction of chromium (VI)

The main results obtained in the photochemical reduction of chromium (VI) reaction are represented in Figure 6. Firstly, a blank reaction under UV-Vis radiation and without a photocatalyst was carried out. During this test, a decrease in the chromium (VI) concentration (i.e., 4.83 %) was observed, which could be caused by a possible reduction of this metal on the glass reactor walls since they changed color after the reaction.

Then, a model reaction in the presence of the photocatalyst without irradiation was also performed. For this test, the material showing the best behavior in the Cr photocatalytic reduction reaction (Pt-S-TiO_2) was selected. This demonstrated that the Cr adsorption on the solid can take place [30], especially because after 5 hours under continuous stirring, the concentration of chromium in the liquid phase decreased by 21.5%.

Likewise, as reported in section 2.2, the adsorption-desorption balance was performed at the start of each reaction with the different materials. The Cr(VI) percentage removal from the fluid phase was very similar for all the photocatalysts, close to 11%, thus indicating similar surface adsorption properties for all materials.

During the photocatalytic reaction, it was possible to determine that when both UV-Vis radiation and photocatalyst are in the reaction medium, the reduction of chromium significantly increases. Thus, as seen in Figure 6, the percentage of Cr (VI) removal is higher after reacting with all the photocatalysts tested.

As observed in Figure 6, during the first 20 minutes of the photocatalytic reaction, there is an important reduction in the concentration of chromium. However, after 30 min, the concentration of this metal had a slight tendency to increase. This behavior can be explained by the possible re-oxidation of chromium. Re-oxidation is mostly due to the competition of H_2O for the holes and hydroxyl radicals such that the reduction of the metal is unfavorable, and the initial oxidation state of the metal species occurs, thus resulting in the desorption of the metal from the TiO_2 surface [30–33].

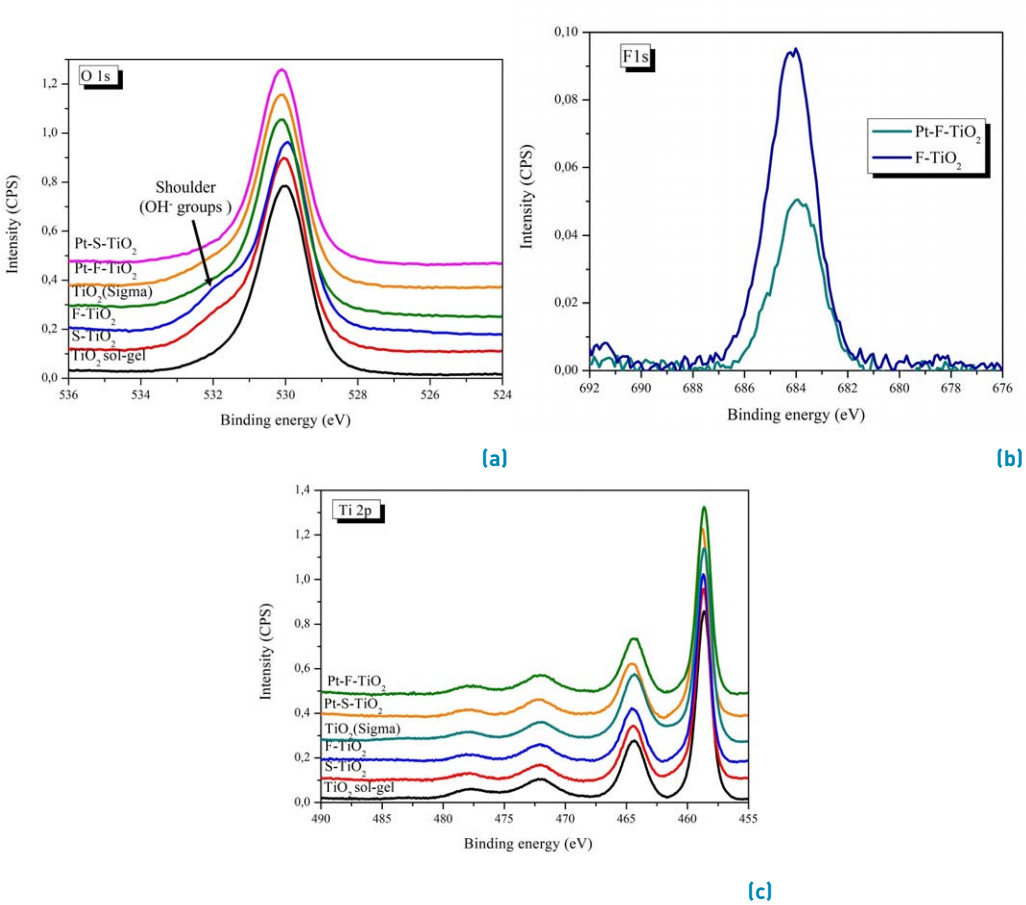

(a) (b) (c)

Figure 4 XPS spectra a) O 1s region, b) F 1s region, c) Ti 2p region

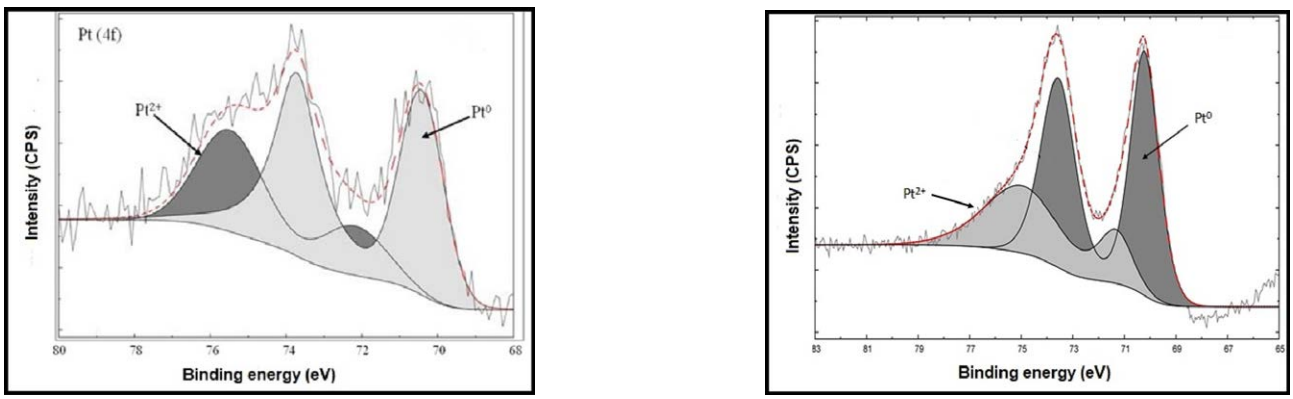

(a) (b)

Figure 5 XPS spectrum of Platinum 4f region for Pt-S-TiO_2. (a) before reaction and (b) after reaction

In general, it was observed that the processes of sulfation, fluoridation, and subsequent addition of platinum improved the photocatalytic activity of the TiO_2 sol-gel, thus leading to an increase in the effectiveness of this oxide in the elimination of Cr (VI) in the reaction medium.

The best performance in the reduction of Cr was observed by using Pt-S-TiO_2 as a photocatalyst after 2 hours of reaction. With this material, the concentration of chromium (VI) decreased up to 82,13%. At the end of the reaction, the Cr (VI) content in the fluid phase was 8.2×10^{-6} mM, equivalent to 0.42 mg/L of Cr (VI), which is lower than the maximum permissible limits given by the Colombian regulation for wastewater and surface water

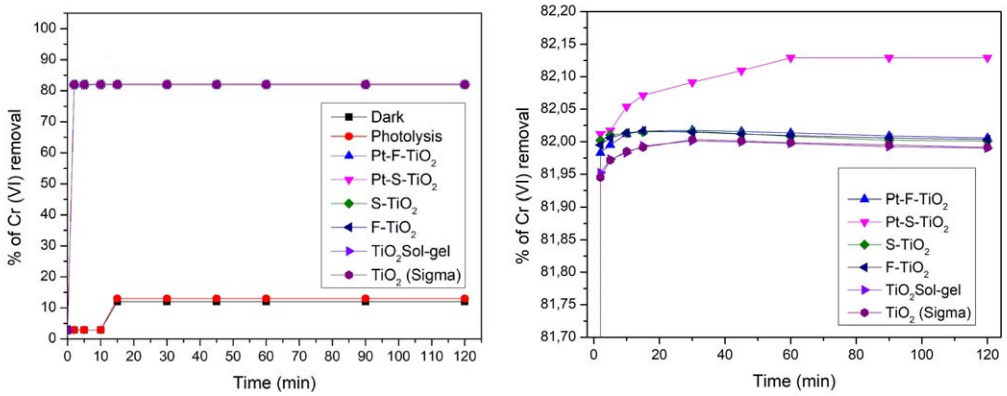

Figure 6 Percentage of Cr (VI) removal, determined by UV-Vis spectrophotometry. a) all reactions. b) Y-axis enlargement

discharges (i.e., 0.50 mg/L) [34, 35]. As seen in Figure 7, only photocatalytic treatment with Pt-S-TiO_2 compliance was achieved by Colombian regulation; however, the second-best performance was achieved with Pt-F-TiO_2 (i.e., 0,52 mg/L Cr (VI)).

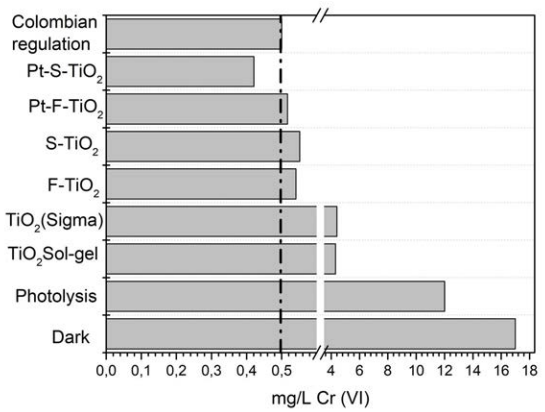

Figure 7 Concentration of Cr (VI) in mg/L after 2 hours of photocatalytic treatment compared Colombian regulation

The top activity observed with Pt-S-TiO_2 in the photoreduction of Cr can be attributed to the physicochemical properties of this material: (i) this material presents a higher surface area than fluoridated material. (ii) Sulfation and Pt addition led to a small reduction in the band gap value compared to TiO_2 sol-gel, thus leading to a decrease in the distance for the promotion of electrons from the valence band to the conduction band in the solid, resulting in a higher reaction efficiency. (iii) Platinized material exhibits absorption in the visible region of the electromagnetic spectrum, thus leading to a better use of the energy. (iv) As observed by TEM analysis, the distribution of Pt nanoparticles was the best and resulted in most of the particles on the surface being able to act effectively as a sink for the photogenerated electrons and increase the electron-hole half-time. (v) The TiO_2 sulfation inhibits the rutile phase formation, thus allowing the anatase phase, which is considered more active in photocatalytic processes, to be favored [17].

As previously indicated in Section 2, the Cr (VI) content was evaluated by UV-Vis spectrophotometry, while the total chromium content in the fluid phase after 2 hours of photocatalytic treatment was studied using atomic absorption spectrometry. Figure 8 represents the concentration of total chromium in the liquid phase at the end of the photocatalytic treatment. As shown in this figure, the final concentration of this metal was 4×10^{-3} mM (2,08mg/L) using Pt-S-TiO_2 and 4.5×10^{-3} mM (2,34mg/L) with Pt-F-TiO_2.

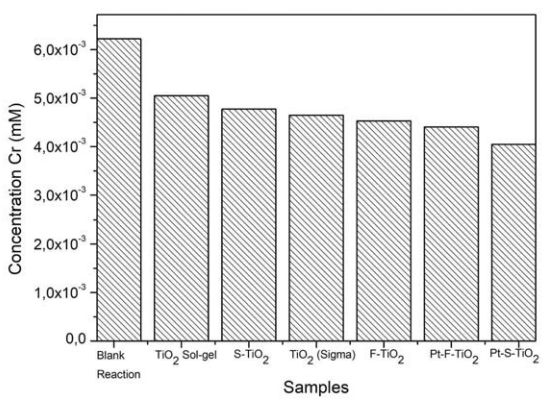

Figure 8 Total chromium concentration measured by atomic absorption spectroscopy in the samples after 2 hours of photocatalytic reaction

The overall trend of photocatalytic was TiO_2 sol-gel $< S{-}TiO_2 < TiO_2$ (Sigma) $<$ F$-$TiO$_2 < Pt{-}F{-}TiO_2 < Pt - S - TiO_2$: this is in good agreement with that

also found by UV-Vis analysis.

In order to determine the oxidation state of chromium deposited on the surface external of photocatalysts analyzed, TiO_2 Sol-gel and Pt-S-TiO_2 were selected to be studied by XPS. These solids were recovered after 2 hours of photocatalytic reaction.

Figure 9 presents the XPS spectra obtained for the Cr $2p_{3/2}$ region; signals are not very clear due to the low chromium content; however, by comparison with theoretical spectra [26], the presence of characteristic signals of Cr^{6+}, Cr^{3+}, and Cr^0 oxidation states was evidenced; these signals are located at 580, 576 and 574 eV, correspondingly. The results obtained show Cr^0 after the reaction, species due to the photocatalytic treatment performed, allowing the Cr photoreduction on the photocatalyst surface. It has been widely reported in the literature that metals can present photochemical reduction, confirming the metallic spices of Cr^0 on the surface of the solid [29, 36].

Best photocatalyst recycling: The stability of the photocatalyst Pt-S-TiO_2 was evaluated by reusing it in four consecutive cycles. The reaction conditions included a light intensity of 120 W/m^2, the presence of nitrogen as an inert gas, constant stirring, and a maximum time of 2 hours. The solid was recovered by filtration and drying at 100°C for 4 hours for use in the next cycle. As evidenced in Figure 10, after the 4th cycle, there was a 30% activity loss compared with the first cycle. This was probably due to the saturation on the surface of the photocatalyst by the reduced chromium species in each of the cycles.

3.3 Evaluation of the impact of reaction parameters on photochemical reduction of chromium

Since the Pt-S-TiO_2 had the best performance in the photoreduction of Cr, this photocatalyst was selected to test the impact of different reaction parameters on the overall effectiveness of this material in the removal of Cr from the liquid phase. Table 2 describes the evaluated reaction conditions.

Table 2 Reaction parameters evaluated in the Cr photoreduction reaction

Reaction parameter	Reaction conditions
Light intensity	Time: 5 hours Light intensity: $30W/m^2$ or $120W/m^2$ Atmosphere: N_2
Reaction time	Time: 2 and 5 hours Light intensity: 120 W/m^2 Atmosphere: N_2
Reaction atmosphere	Time: 5 hours Light intensity: $30W/m^2$ Atmosphere: O_2 or N_2

Light intensity effect: As shown in Figure 11, it was found that an increase in light intensity from 30 to $120W/m^2$ led to a higher effectiveness in the removal of Cr. This is mainly due to a higher photonic efficiency, which increases the energy available for the photocatalytic process.

Reaction time effect: It was also found that an increase in reaction time from 2 to 5 hours led to an increase in the concentration of chromium in the fluid phase. This is because, in the reaction medium, the Cr (III) species can compete with $H2_O$ for hydroxyl radicals and holes. As a result, the photoreduction of the metal is at a disadvantage, and the initial oxidation state of chromium is regenerated, as seen in Equation 1 [37, 38]; then, a desorption of the Cr from the outside of TiO_2 can occur.

$$\mathrm{Cr(III)} \xrightarrow{h^+_{BV}/\mathrm{HO}} \mathrm{Cr(IV)} \xrightarrow{h^+_{BV}/\mathrm{HO}} \mathrm{Cr(V)} \xrightarrow{h^+_{\mathrm{VV}}/\mathrm{HO}} \mathrm{Cr(VI)} \quad (1)$$

Reaction atmosphere effect: It was found that with the reaction parameters used in this study, the reaction atmosphere (nitrogen or oxygen) did not significantly modify the reduction of Cr.

4. Conclusions

The materials synthesized were based on TiO_2 and modified by sulfation, fluoridation, and subsequent platinization, which allowed the physicochemical properties of the final photocatalysts obtained to be controlled. The main differences observed in the materials synthesized were: (i) after modification, only the crystalline phase Anatase was obtained, thus avoiding the rutile formation, and (ii) after fluoridation and platinization, absorption in the visible region of the electromagnetic spectrum was favored.

The best photochemical reduction of chromium was obtained using Pt-S-TiO_2 as a photocatalyst, under continuous stirring, N_2 atmosphere, a light intensity of 120 W/m^2, and 2 hours of final reaction time; these lab conditions are the starting point for a possible scaling up of the process.

The highest effectiveness from the photocatalyst Pt-S-TiO_2 in the photoreduction of Cr can be explained as a synergic effect as a function of its physicochemical properties such as a high specific surface area, a slight reduction in bandwidth, homogeneous distribution of Pt nanoparticles, and a greater hydroxylation on the surface compared Pt-F-TiO_2.

Heterogeneous photocatalysis based on TiO_2 was found to be a suitable method for the removal of chromium

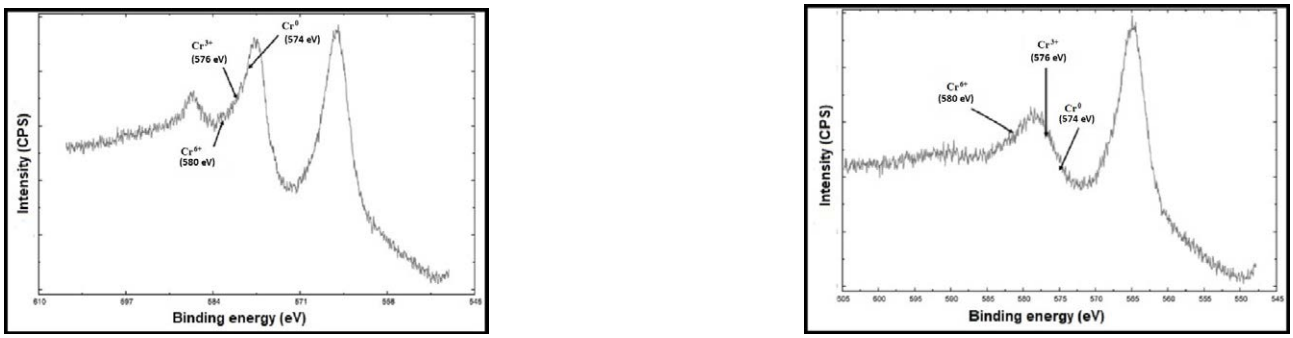

Figure 9 XPS spectra for Cr 2p3/2 region after photocatalytic reaction. a) Pt-S-TiO_2 and b) TiO_2 Sol-gel

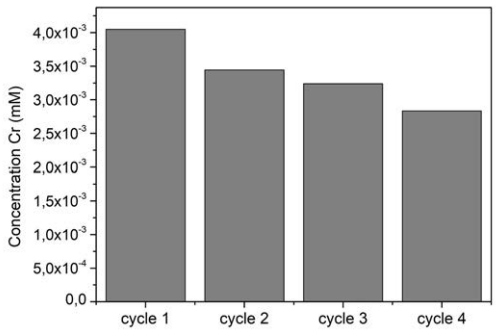

Figure 10 Total chromium of consecutive cycling

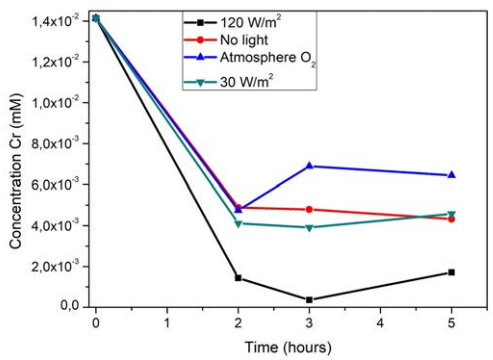

Figure 11 Effect of different experimental parameters evaluated in the Cr removal by photocatalytic reduction on Pt-S-TiO_2

(VI), which is present in effluents. These powders allow the photochemical reduction of chromium on the photocatalyst surface, which leads to efficient removal of this pollutant from the liquid phase, complying with the Colombian regulations of wastewater discharge for Cr (VI). However, the reaction time is a factor to be controlled: it is because it was observed that an increase above 2 h of total reaction time had a detrimental effect on the efficiency of Cr removal, which can be due to a re-oxidation and desorption of the metal from the photocatalyst surface.

5. Declaration of competing interest

We declare that we have no competing interests, including financial or non-financial, professional, or personal interests, interfering with the full and objective presentation of the work described in this manuscript.

6. Acknowledgments

M. Hernández-Laverde would like to thank Ministerio de Ciencia Tecnología e Innovación de Colombia (Minciencias) and Gobernación de Boyacá for the concession of a researcher grant (OCAD- Fondo Nacional de Financiamiento para la Ciencia, la Tecnología e Innovación (FCTel) del Sistema general de regalías, Becas de Excelencia Doctoral del Bicentenario).

7. Funding

This work was funded by the Ministerio de Ciencia, Tecnología e Innovación – Minciencias and Ministerio de Salud y Protección Social, Project 110991891727-2020, and Universidad Pedagógica y Tecnológica de Colombia (UPTC) Project SGI 3393. Part of these results have been funded by the Reference Project PID2021-122413NB-I00 in the area of Environmental Sciences and Technologies in the framework of the Knowledge Generation Projects 2021 (Ministry of Science and Innovation, Spain), which is gratefully acknowledged.

8. Author contributions

Julie Joseane Murcia Mesa provided the main idea, revised of the manuscript and acquisition of the financial support

for the project, Mónica Sirley Hernández Laverde prepared the manuscript (Writing-preparation of the original draft) and data collection of investigation. Ivan Alexander Correa Camargo performed specifically the experiments. Hugo Alfonso Rojas Sarmiento revised the idea of the manuscript providing suggestions and acquisition of the financial support for the project. José Antonio Navío and María del Carmen Hidalgo López have contributed in the characterization of photocatalytic materials in the Investigation.

Julie Joseane Murcia Mesa provided the main idea, revised of the manuscript and acquisition of the financial support for the project, Mónica Sirley Hernández Laverde prepared the manuscript (Writing-preparation of the original draft) and data collection of investigation. Ivan Alexander Correa Camargo performed specifically the experiments. Hugo Alfonso Rojas Sarmiento revised the idea of the manuscript providing suggestions and acquisition of the financial support for the project. José Antonio Navío and María del Carmen Hidalgo López have contributed in the characterization of photocatalytic materials in the Investigation. where the data associated with a paper is available, and under what conditions the data can be accessed. They also include links (where applicable) to the data set.

References

[1] F. Fu and Q. Wang, "Removal of heavy metal ions from wastewaters: a review," *Journal of Environmental Management*, vol. 92, no. 3, Dec. 07, 2010. [Online]. Available: https://doi.org/10.1016/j.jenvman.2010.11.011

[2] B. Henry, J. M. Vásquez, J. Moscoso-Cavallini, S. Oakley, L. Salguero, and P. Saravia. (2011) Tratamiento de aguas residuales domésticas en centroamérica. Acuerdo de cooperación USAID-CCAD. [Online]. Available: https://www.academia.edu/download/52717324/Manual_Aguas_residuales.pdf

[3] R. Sarria-Villa, J. Gallo-Corredor, and R. Benítez-Benítez, "Tecnologías para remover metales pesados presentes en aguas. caso cromo y mercurio," *Journal de Ciencia e Ingeniería*, vol. 12, no. 1, Jun. 11, 2020. [Online]. Available: https://doi.org/10.46571/JCI.2020.1.8

[4] Y. Ibrahim, E. Abdulkarem, V. Naddeo, F. Banat, and S. Hasan, "Synthesis of super hydrophilic cellulose-alpha zirconium phosphate ion exchange membrane via surface coating for the removal of heavy metals from wastewater," *Science of The Total Environment*, vol. 690, Jul. 03, 2019. [Online]. Available: https://doi.org/10.1016/j.scitotenv.2019.07.009

[5] N. Qasem, R. Mohammed, and D. Lawal, "Removal of heavy metal ions from wastewater: A comprehensive and critical review," *npj Clean Water*, vol. 4, no. 36, Jul. 08, 2021. [Online]. Available: https://doi.org/10.1038/s41545-021-00127-0

[6] T. Kośla, M. Skibniewski, E. M. Skibniewska, I. Lasocka, and M. Kołnierzak, "Molybdenum, mo," in *Mammals and Birds as Bioindicators of Trace Element Contaminations in Terrestrial Environments*, E. Kalisińska, Ed. Switzerland, AG: Springer, Cham., 2019. [Online]. Available: https://doi.org/10.1007/978-3-030-00121-6_8

[7] J. Hojman, J. Meichtry, M. Litter, and C. Coll, "Abatement of toxicity of effluents containing cr (vi) by heterogeneous photocatalysis. toxicity assessment by amphitox assay," *Ecotoxicology and Environmental Safety*, vol. 122, Sep. 29, 2015. [Online]. Available: https://doi.org/10.1016/j.ecoenv.2015.09.036

[8] M. Litter, "Mechanisms of removal of heavy metals and arsenic from water by TiO_2-heterogeneous photocatalysis," *Pure and Applied Chemistry*, vol. 87, no. 6, Jan. 10, 2015. [Online]. Available: https://doi.org/10.1515/pac-2014-0710

[9] J. Liu, Q. Liu, J. Li, X. Zheng, Z. Liu, and X. Guan, "Photochemical conversion of oxalic acid on heterojunction engineered $FeWO_4$/g-C_3N_4 photocatalyst for high-efficient synchronous removal of organic and heavy metal pollutants," *Journal of Cleaner Production*, vol. 363, Jan. 09, 2022. [Online]. Available: https://doi.org/10.1016/j.jclepro.2022.132527

[10] K. Quiton, M. Lu, and Y. Huang, "Synthesis and catalytic utilization of bimetallic systems for wastewater remediation: A review," *Chemosphere*, vol. 262, Sep. 18, 2020. [Online]. Available: https://doi.org/10.1016/j.chemosphere.2020.128371

[11] O. Sacco, J. Murcia, A. Lara, M. Hernández-Laverde, H. Rojas, J. Navío, and *et al.*, "Pt–TiO_2–Nb_2O_5 heterojunction as effective photocatalyst for the degradation of diclofenac and ketoprofen," *Materials Science in Semiconductor Processing*, vol. 107, Nov. 21, 2019. [Online]. Available: https://doi.org/10.1016/j.mssp.2019.104839

[12] E. Kumar, T. Wang, H. Chi, and Y. Chang, "Hydrothermal and photoreduction synthesis of nanostructured $\alpha - Fe_2O_3/Ag$ urchins for sensitive SERS detection of environmental samples," *Applied Surface Science*, vol. 604, Aug. 05, 2022. [Online]. Available: https://doi.org/10.1016/j.apsusc.2022.154448

[13] P. Kajitvichyanukul, J. Ananpattarachai, and S. Pongpom, "Sol–gel preparation and properties study of TiO_2 thin film for photocatalytic reduction of chromium(VI) in photocatalysis process," *Science and Technology of Advanced Materials*, vol. 6, no. 3-4, 2005. [Online]. Available: https://doi.org/10.1016/j.stam.2005.02.014

[14] Y. Ku and I. Jung, "Photocatalytic reduction of cr (vi) in aqueous solutions by uv irradiation with the presence of titanium dioxide," *Water Research*, vol. 35, no. 1, Nov. 14, 2000. [Online]. Available: https://doi.org/10.1016/S0043-1354(00)00098-1

[15] R. Lakra, M. Kiran, and P. Korrapati, "Furfural mediated synthesis of silver nanoparticles for photocatalytic reduction of hexavalent chromium," *Environmental Technology & Innovation*, vol. 21, Dec. 29, 2020. [Online]. Available: https://doi.org/10.1016/j.eti.2020.101348

[16] R. Djellabi, F. Ghorab, S. Nouacer, A. Smara, and O. Khireddine, "Cr(VI) photocatalytic reduction under sunlight followed by Cr(III) extraction from TiO_2 surface," *Materials Letters*, vol. 176, Apr. 11, 2016. [Online]. Available: https://doi.org/10.1016/j.matlet.2016.04.090

[17] K. Vikrant and S. Weon and K.H. Kim and M. Sillanpää, "Platinized titanium dioxide (Pt/TiO_2) as a multi-functional catalyst for thermocatalysis, photocatalysis, and photothermal catalysis for removing air pollutants," *Applied Materials Today*, vol. 23, Mar. 05, 2021. [Online]. Available: https://doi.org/10.1016/j.apmt.2021.100993

[18] J. Mesa, M. Laverde, H. Sarmiento, M. Angulo, J. Navío, and M. López, "Cómo el precursor de Ti está involucrado en la eficacia de los materiales Pt-TiO_2 en la fotodegradación de metil naranja," *Revista Facultad de Ciencias Básicas*, vol. 16, no. 2, 2020. [Online]. Available: https://doi.org/10.18359/rfcb.5013

[19] J. Murcia, M. Hernández-Laverde, H. Rojas, E. Muñoz, J. Navío, and M. Hidalgo, "Study of the effectiveness of the flocculation-photocatalysis in the treatment of wastewater coming from dairy industries," *Journal of Photochemistry and Photobiology A: Chemistry*, vol. 358, Mar. 21, 2018. [Online]. Available: https://doi.org/10.1016/j.jphotochem.2018.03.034

[20] J. Murcia, A. Cely, H. Rojas, M. Hidalgo, and J. Navío, "Fluorinated and platinized titania as effective materials in the photocatalytic treatment of dyestuffs and stained wastewater coming from handicrafts factories," *Catalysts*, vol. 9, no. 2, Feb. 14, 2019. [Online]. Available: https://doi.org/10.3390/catal9020179

[21] G. Iervolino, V. Vaiano, J. Murcia, L. Rizzo, G. Ventre, G. Pepe, and *et al.*, "Photocatalytic hydrogen production from degradation

of glucose over fluorinated and platinized TiO_2 catalysts," *Journal of catalysis*, vol. 339, Apr. 18, 2016. [Online]. Available: https://doi.org/10.1016/j.jcat.2016.03.032

[22] *Standard Test Methods for Chromium in Water*, ASTM D1687-12, 2017.

[23] W. G. Walter, "Standard methods for the examination of water and wastewater (11th ed.)," *Home American Journal of Public Health (AJPH)*, vol. 51, no. 6, Jun. 01, 1961. [Online]. Available: https://doi.org/10.2105/AJPH.51.6.940-a

[24] A. Kubiak, N. Varma, and M. Sikorski, "Insight into the led-assisted deposition of platinum nanoparticles on the titania surface: understanding the effect of leds," *Scientific Reports*, vol. 12, Dec. 29, 2022. [Online]. Available: https://doi.org/10.1038/s41598-022-27232-5

[25] H. Park, Y. Park, W. Kim, and W. Choi, "Surface modification of TiO_2 photocatalyst for environmental applications," *Journal of Photochemistry and Photobiology C: Photochemistry Reviews*, vol. 15, Nov. 15, 2012. [Online]. Available: https://doi.org/10.1016/j.jphotochemrev.2012.10.001

[26] T. Yamaki, T. Umebayashi, T. Sumita, S. Yamamoto, M. Maekawa, A. Kawasuso, and *et al.*, "Fluorine-doping in titanium dioxide by ion implantation technique," *Nuclear Instruments and Methods in Physics Research Section B: Beam Interactions with Materials and Atoms*, vol. 206, Feb. 12, 2003. [Online]. Available: https://doi.org/10.1016/S0168-583X(03)00735-3

[27] A. Sobczyk-Guzenda, S. Owczarek, A. Wojciechowska, D. Batory, M. Fijalkowski, and M. Gazicki-Lipman, "Fluorine doped titanium dioxide films manufactured with the help of plasma enhanced chemical vapor deposition technique," *Thin Solid Films*, vol. 650, Feb. 01, 2018. [Online]. Available: https://doi.org/10.1016/j.tsf.2018.01.060

[28] P. Connor, K. Dobson, and A. McQuillan, "Infrared Spectroscopy of the TiO_2/Aqueous Solution Interface," *Langmuir*, vol. 15, no. 7, Mar. 02, 1999. [Online]. Available: https://doi.org/10.1021/la980855d

[29] M. Hidalgo, M. Maicu, J. Navío, and G. Colón, "Study of the synergic effect of sulphate pre-treatment and platinisation on the highly improved photocatalytic activity of TiO_2," *Applied Catalysis B: Environmental*, vol. 81, no. 1-2, Dec. 08, 2007. [Online]. Available: https://doi.org/10.1016/j.apcatb.2007.11.036

[30] J. J. Murcia-Mesa, C. G. Patiño-Castillo, H. A. Rojas-Sarmiento, J. A. Navío-Santos, M. del C. Hidalgo-López, and A. A. Botero, "Photocatalytic treatment based on TiO_2 for a coal mining drainage," *Revista Facultad de Ingeniería, Universidad de Antioquia*, no. 107, Oct. 13, 2021. [Online]. Available: https://doi.org/10.17533/udea.redin.20211063

[31] M. Litter, "Heterogeneous photocatalysis: transition metal ions in photocatalytic systems," *Applied catalysis B: environmental*, vol. 23, no. 2-3, Oct. 11, 1999. [Online]. Available: https://doi.org/10.1016/S0926-3373(99)00069-7

[32] C. Wang, X. Du, J. Li, X. Guo, P. Wang, and J. Zhang, "Photocatalytic cr (vi) reduction in metal-organic frameworks: A mini-review," *Applied Catalysis B: Environmental*, vol. 193, Apr. 19, 2016. [Online]. Available: https://doi.org/10.1016/j.apcatb.2016.04.030

[33] E. Wahyuni, N. Aprilita, H. Hatimah, A. Wulandari, and M. Mudasir, "Removal of toxic metal ions in water by photocatalytic method," *American Chemical Science Journal*, vol. 5, no. 2, Nov. 15, 2014. [Online]. Available: https://doi.org/10.9734/ACSJ/2015/13807

[34] *Por la cual se establecen los parámetros y los valores límites máximos permisibles en los vertimientos puntuales a cuerpos de aguas superficiales y a los sistemas de alcantarillado público y se dictan otras disposiciones*, Resolución N° 0631, Under Ministerio de Ambiente y Desarrollo Sostenible, Bogotá, CO, 2015. [Online]. Available: https://www.minambiente.gov.co/wp-content/uploads/2021/11/resolucion-631-de-2015.pdf

[35] *Derogado por el art. 79, Decreto Nacional 3930 de 2019, salvo los arts. 20 y 21. Por el cual se reglamenta parcialmente el Título I de la Ley 09 de 1979, así como el Capítulo II del Título VI-Parte III - Libro II y el Título III de la Parte III Libro I del Decreto 2811 de 1974 en cuanto a usos del agua y residuos líquidos*, Decreto 1594, Under Ministerio de Comercio, Industria y Turismo, Bogotá, CO, 1984. [Online]. Available: https://www.mincit.gov.co/ministerio/normograma-sig/procesos-de-apoyo/gestion-de-recursos-fisicos/decretos/decreto-1594-de-1984.aspx

[36] Y. Sun, Z. Liu, Y. Zhang, L. Han, and Y. Xu, "Highly porous ZnO modified with photochemical deposition of silver nanostructure for ultra-sensitive triethylamine detection," *Sensors and Actuators B: Chemical*, vol. 391, May. 25, 2023. [Online]. Available: https://doi.org/10.1016/j.snb.2023.134027

[37] G. Chiarello, M. Dozzi, M. Scavini, J. Grunwaldt, and E. Selli, "One step flame-made fluorinated Pt/TiO_2 photocatalysts for hydrogen production," *Applied Catalysis B: Environmental*, vol. 160-161, May. 10, 2014. [Online]. Available: https://doi.org/10.1016/j.apcatb.2014.05.006

[38] A. Sheoran and V. Sheoran, "Heavy metal removal mechanism of acid mine drainage in wetlands: a critical review," *Minerals engineering*, vol. 19, no. 2, Oct. 04, 2005. [Online]. Available: https://doi.org/10.1016/j.mineng.2005.08.006